Atmospheric
Chemistry
and Physics
Discussions
EGU

The Production and Hydrolysis of Organic Nitrates from OH Radical Oxidation of β-Ocimene

Ana C. Morales[1,*], Thilina Jayarathne[1,a,*], Jonathan H. Slade[2], Alexander Laskin[1,3], and Paul B. Shepson[1,3,4]

[1]Department of Chemistry, Purdue University, West Lafayette, IN 47906, USA
[2]Department of Chemistry & Biochemistry, University of California San Diego, La Jolla, CA 92093, USA
[3]Department of Earth, Atmospheric, and Planetary Sciences, Purdue University, West Lafayette, IN 47906, USA
[4]School of Marine and Atmospheric Sciences, Stony Brook University, Stony Brook, NY 11794, USA
[a]now at: Bristol Myers Squibb, 1 Squibb Drive, New Brunswick, NJ 08901, USA
[*]These two authors equally contributed for this work

Correspondence to: paul.shepson@stonybrook.edu

Abstract. Biogenic volatile organic compounds (BVOCs) emitted by plants represent the largest source of non-methane hydrocarbon emissions on Earth. Photochemical oxidation of BVOCs represents a significant pathway in the production of secondary organic aerosol (SOA), affecting Earth's radiative balance. Organic nitrates ($RONO_2$), formed from the oxidation of BVOCs in the presence of NO_x, represent important aerosol precursors, and affect the oxidative capacity of the atmosphere, in part by sequestering NO_x. In the aerosol phase, $RONO_2$ hydrolyze to form nitric acid and numerous water-soluble products, thus contributing to an increase in aerosol mass. However, only a small number of studies have investigated the production of $RONO_2$ from •OH oxidation of terpenes, among those, few have studied their hydrolysis. Here, we report a laboratory study of OH radical-initiated oxidation of β-ocimene, an acyclic, triolefinic monoterpene released during the daytime from vegetation, including forests, agricultural landscapes, and grasslands. We conducted studies of the OH radical oxidation of β-ocimene in the presence of NO_x using a 5.5 m^3 all-Teflon photochemical reaction chamber, during which we quantified the total (gas- and particle-phase) $RONO_2$ yield and the SOA yields. We sampled the organic nitrates produced and measured their hydrolysis rate constants at different solution pH. The total organic nitrate yield was determined to be 33($\pm$7)%, consistent with the available literature regarding the

dependence of organic nitrate production (from RO_2 + NO) on carbon number. We found the hydrolysis rate constants to be highly pH-dependent, with a hydrolysis lifetime of 51($\pm$13) min at pH=4, and 24($\pm$3) min at pH = 2.5, a typical pH for deliquesced aerosols. We also employed high-resolution mass spectrometry for product identification, which is used to infer key mechanisms of gas–particle partitioning. The results indicate that the ocimene SOA yield under relevant aerosol mass loadings in the atmosphere is significantly lower (<1%) than reported yields from cyclic terpenes, such as α-pinene, likely due to alkoxy radical decomposition and formation of smaller higher-volatility products. This is also consistent with the observed lower particle-phase organic nitrate yields of β-ocimene, 1.5($\pm$0.5)%, under dry conditions. We observed the expected hydroxy nitrates by chemical ionization mass spectrometry (CIMS), and some secondary production of the di-hydroxy di-nitrates, likely produced by oxidation of the first-generation hydroxy nitrates. Lower $RONO_2$ yields were observed under high relative humidity (RH) conditions, indicating the importance of aerosol-phase $RONO_2$ hydrolysis under ambient RH. This study provides insight into the formation and fate of organic nitrates, ocimene SOA yields, and NO_x cycling in forested environments from daytime monoterpenes, which are not currently included in atmospheric models.

1 Introduction

Biogenic volatile organic compounds (BVOCs) constitute the largest flux (88%) of all non-methane organic compounds to the atmosphere (Goldstein and Galbally, 2007; Guenther et al., 1995, 2012). Isoprene and monoterpenes account for ~60% of the total global BVOC emissions (Goldstein and Galbally, 2007; Guenther et al., 1995). BVOCs participate in chemical reactions with criteria air pollutants, including NO_x and O_3, and with radical species such as OH and NO_3, which leads to the formation of low volatility oxygenated compounds that partition into aerosol particles and represent a source of secondary organic aerosol (SOA) (Atkinson and Arey, 2003; Hallquist et al., 2009; Hatakeyama et al., 1991; Isaksen et al., 2009; Lee et al., 2016; Monks et al., 2009; Perring et al., 2013; Pye et al., 2015). Globally, the oxidation of BVOCs emitted from forests represents the largest source of SOA and affect climate and air quality. (Hallquist et al., 2009).

55   One specific group of BVOC oxidation products of interest is the organic nitrates ($RONO_2$). By sequestering NO_x, $RONO_2$ slows the production of tropospheric O_3, but can act as a source of NO_x and O_3 downwind upon further oxidation (Browne and Cohen, 2012; Pusede et al., 2015). These low volatility, water-soluble compounds are important precursors to and constituents of SOA due to their efficient partitioning with the condensed-phase (Biesenthal et al., 1997; Fry et al., 2009, 2014; Perraud et al., 2012;

60   Rollins et al., 2012). Ambient measurements have indicated that up to 23% of molecules in organic aerosol contain the $RONO_2$ functional group, suggesting $RONO_2$ represent a significant fraction of BVOC-derived oxidation products (Ditto et al., 2020; Rollins et al., 2013). However, the hydrolysis lifetime in the aerosol phase (~1-3 hours) is much shorter than the lifetime of the aerosol itself (~1 week), which suggests the contribution of organic nitrates to aerosol mass may have been underestimated from

65   the observational data (Romer et al., 2016).

It has been shown that these low-volatility oxidation products readily partition from the gas phase into the particle phase and undergo further reactions (Perraud et al., 2012). Once in the particle phase, organic nitrates can undergo rapid hydrolysis under acid-catalyzed conditions, representing a sink for NO_x in the form of HNO_3 (Bean and Hildebrandt Ruiz, 2016; Darer et al., 2011; Hu et al., 2011; Liu et

70   al., 2012; Rindelaub et al., 2015; Takeuchi and Ng, 2019). Hydrolysis rates and the relative contribution of particle phase hydrolysis as a sink for organic nitrates (compared to reaction with ozone, OH, photolysis, and deposition) vary significantly and depend on molecular structure (Boyd et al., 2015; Zare et al., 2018). To date, there are few studies of hydrolysis rate constants for monoterpene-derived organic nitrates (Rindelaub et al., 2015). The chemical structure (primary, secondary, and tertiary) can influence

75   the rate of hydrolysis of organic nitrates (Boyd et al., 2015; Zare et al., 2018). Thus, more studies are needed to assess the structural dependence of both $RONO_2$ production yields and the hydrolysis rate constants.

Although monoterpenes contribute significantly to the total annual BVOC budget, current models underestimate the impact of $RONO_2$ on SOA mass measured in an ambient environment (Pye et al., 2013).

80   Importantly, $RONO_2$ yields for many BVOCs are unknown. Monoterpenes have been shown to produce more SOA than from isoprene in boreal regions (Lee et al., 2006; Tsigaridis and Kanakidou, 2007). Pratt et al. (2012) showed that, for a temperate mixed-forest in Michigan, isoprene-derived nitrates dominate

Atmospheric
Chemistry
and Physics
Discussions

Open Access

EGU

the daytime simulated gas-phase organic nitrates, however, ~20% is derived from monoterpene nitrates. Of this, nearly one third results from OH-initiated oxidation of β-ocimene, a tri-olefinic monoterpene of high reactivity that is emitted during the daytime (Pratt et al., 2012). To the best of our knowledge, the production of β-ocimene organic nitrates and aqueous-phase processing of its atmospheric oxidation products have not previously been studied.

To expand our understanding of the chemical evolution and fate of monoterpene-derived $RONO_2$, we investigated the formation of $RONO_2$ produced from the •OH-initiated oxidation of ocimene in the presence of NO_x using a photochemical reaction chamber. These experiments were conducted as a function of chamber RH to provide insight on aqueous phase partitioning and processing. The aqueous phase processing of these species was explored using linear quadrupole ion trap mass spectrometry to determine hydrolysis kinetics. This study aims to quantify the yields of ocimene-derived $RONO_2$ and the chemistry of these species to better understand how organic nitrates may impact air quality and climate.

2 Methods

Experiments were conducted in a custom-made, 5.5 m^3 photochemical reaction chamber consisting of PFA-Teflon walls, perfluoroalkoxy-coated endplates, a mixing fan, and UV lamps as described in Chen et al., 1998 and Lockwood et al., 2010. These experiments were conducted as a function of chamber RH, keeping other variables constant as possible, and at ~25°C. Eighteen experiments were carried out under variable humidity conditions, i.e. <3% up to 70% RH, as listed in Table 1.

Before the experiment, the chamber walls were cleaned by adding ~500 ppb O_3, irradiating for 1 hour, and flushing with ultra-zero (UZ) air in the dark until the O_3 concentration was ~0 ppb. The O_3 concentration was monitored using a dual beam ozone monitor (2B Technologies, model 205), which is calibrated using an ozone calibration source (2B technologies, model 306). The chamber RH was monitored using a LI-COR hygrometer (model 7000). The LI-COR was calibrated from known RH sampled over a saturated K_2SO_4 solution at a fixed temperature. Experiments were started only if the chamber particle number concentration was <10 particles per cubic centimeter.

First, ocimene (≥90%, Sigma-Aldrich; (*E*)-/(*Z*)-β-ocimene mixture) was introduced to the chamber via injection through a T-shaped heated glass inlet, through which ultrapure N_2 was used to

Atmospheric
Chemistry
and Physics
Discussions

Open Access

EGU

110   transfer the injected ocimene via 1/4″ PFA tubing at a flowrate of 5 lpm. Formaldehyde (37% v/v in water,

Sigma) and pure NO (99.5%, Praxair) were injected using the same set-up. Formaldehyde photolysis

serves as an OH radical precursor in the presence of NO (Possanzini et al., 2002). Ammonium Sulfate

$((NH_4)_2SO_4)$ seed particles were generated using a 10 wt.% $(NH_4)_2SO_4$ aqueous solution and a

commercial atomizer (TSI, Inc., model 3076), and subsequently dried by passing through a diffusion

115   dryer prior to entering the reaction chamber. For humid experiments, chamber RH was adjusted by

bubbling UZ air through nano-pure water using a commercial bubbler immersed in a temperature-

controlled bath. The chamber fan was started during the initial injections, ensuring reactants were well

mixed. Following mixing, initial concentrations were measured before the chamber UV lights were

activated. After initial concentrations were measured, the fan was stopped to minimize wall losses, the

120   chamber lights were activated (time = 0), and real-time measurements were obtained. A representative

experimental time series is shown in Figure 1, where the area between the blue vertical lines represents

the time when the UV lights were switched on.

The ocimene concentration was quantified using gas chromatography – flame ionization detection

(GC-FID; HP 5890 Series II) equipped with a gas injection loop. The GC-FID was calibrated using the

125   same ocimene standard injected during the experiments, with gas phase concentrations prepared in ~200-

liter PFA-Teflon bags. Seven-point calibration curves with $R^2 > 0.995$ were obtained and used for

ocimene quantitation. NO and NO_2 concentrations were measured using a custom-built

chemiluminescence NO_x analyzer (Lockwood et al., 2010). Size-resolved particle mass concentration was

determined using a scanning mobility particle sizer (SMPS, TSI, Inc., model 3062) directly connected to

130   the chamber via copper sampling lines. The hydroxy nitrates were quantified using I^- chemical ionization

mass spectrometry (CIMS) (Xiong et al., 2015, 2016). The inlet of the CIMS was maintained at a high

relative humidity via saturated UHP N_2 carrier flow to eliminate the effects of water vapor on the CIMS

sensitivity (Lee et al., 2016; Xiong et al., 2015). A synthesized α-pinene hydroxy nitrate standard was

used as a surrogate standard to calibrate the CIMS for ocimene hydroxy nitrate determination (Rindelaub

135   et al., 2016b; Slade et al., 2017). O_3 measurements were not possible due to interference of the ozone

monitor by ocimene (Walker and Hawkins, 1952). However, for the NO and NO_2 concentrations present

in the chamber, and the J_{NO2} value (7×10^{-4} s^{-1}), the calculated steady state O_3 concentration was < 1 ppb

Atmospheric
Chemistry
and Physics
Discussions

Open Access
EGU

(considering loss via reaction with NO and ocimene) and was not an important reactant in the experiments. The photochemical reaction was terminated by turning off the chamber lights when one third of the NO

140   concentration remained in the chamber to ensure that ocimene oxidation occurred via •OH oxidation only, and all RO_2 radicals reacted only with NO (Atkinson et al., 2006; Capouet et al., 2004; Rindelaub et al., 2015). A series of blank experiments was conducted to evaluate i) chamber reactions without ocimene or NO, ii) gas- and particle-phase product loss to chamber walls under different RH, and iii) dark reactions of NO_2 with ocimene. These blank experiments served as a confirmation that all the $RONO_2$ detected

145   during oxidation experiments were produced from the OH-initiated oxidation in the presence of NO. Additionally, the SOA, gas-, and particle-phase yields were all corrected for the product loss to chamber walls.

      The gas- and particle-phase products were separated and collected for offline analysis by sampling through a XAD-4 resin coated 8 channel annular denuder (URG-200) followed by a 47 mm PTFE particle

150   filter. A series of quality control experiments was performed to evaluate the gas-phase organic nitrate collection efficiency by the denuder, particle transmission efficiency through the denuder, and particle collection efficiency on the filter, as described in Slade et al., 2017. The denuder and filter were separately extracted in tetrachloroethlyene (≥99.9%, Sigma-Aldrich) and subsequently analyzed for total organic nitrate concentration using Fourier transform infrared spectroscopy (FTIR, Thermo Nicolet 6700) using

155   a 1.00 cm liquid cell, as described by Rindelaub et al., 2015. The organic nitrate concentrations were determined using the asymmetric $-ONO_2$ stretch at 1640 cm^{-1} (Nielsen et al., 1995), using an absorption coefficient of 12900 L $mole^{-1}$ cm^{-1}. After the FTIR analysis, samples were concentrated to near-complete dryness with ultra-high-purity nitrogen for use in high resolution mass spectrometry analysis for structure elucidation and hydrolysis studies.

160   To better understand the oxidation products, denuder and filter extracts were analyzed for their chemical composition via ultra-high-performance liquid chromatography with electrospray ionization time-of-flight tandem mass spectrometry (UPLC-ESI-ToF-MS/MS, Sciex 5600+ TripleToF with Shimadzu 30 series pumps and autosampler) (Slade et al., 2017). The separation was achieved using reverse-phased liquid chromatography (Phenomenex Kinetex EVO C18 column, 100 Å, 100 mm × 2.1

165   mm, 5 μm) following the gradient elution described in Surratt et al., 2008, and MS analyses were

completed using negative and positive electrospray ionization (ESI) modes with multiple-reaction monitoring (MRM) in the W reflectron geometry mode. The mass resolution (m/Δm) of this mass spectrometer is 25,000 at m/z 195 using an accumulation time of 50 ms. The denuder and filter extracts were reconstituted in a 1:1 v:v solvent mixture of HPLC-grade methanol with 0.1% acetic acid and HPLC-grade water. The gradient elution was performed at 0.3 mL min^{-1} with a binary mobile phase system: (A) 0.1% acetic acid in water (B) 0.1% acetic acid in methanol. The 12 min gradient elution was as follows: the concentration of eluent B was 0% for the first 2 min, increased to 90% from 2 to 10 min, held at 90% from 10 to 10.2 min, and then decreased back to 0% from 10.2 to 12 min (Surratt et al., 2008).

For hydrolysis studies, 3 experiments were selected representing dry, mid, and high RH conditions. The denuder and filter extracts were combined to form a bulk (gas- and particle-phase) ocimene nitrate solution and was then concentrated by solvent evaporation. The mixture was then reconstituted in 2.0 mL of a buffer solution at pH = 2.5, 4.1, and 7.0. The solution was agitated using a magnetic stir bar and 50 µL were extracted every 2 minutes. The extract was then mixed with 50 µL of methanol (99.9%, Fisher Chemical). The resulting solution was stirred and analyzed via direct infusion electrospray ionization (ESI) into a Thermo Scientific LTQ XL Linear Ion Trap mass spectrometer operated in negative ionization mode. The hydrolysis rate constants were determined from the first-order decay of various organic nitrate-related functional groups monitored by MS^2 fragmentation experiments. Briefly, fragmentation of the isolated molecular ion m/z 214.1 ($C_{10}H_{16}NO_4$, expected first-generation oxidation product) was monitored at the instrument setting of collisional dissociation energy (CE) of 35 eV. The m/z 46 (NO_2^-) and 62 (NO_3^-) mass fragments were used to quantify relative concentrations of $C_{10}H_{16}NO_4$ species as a function of the hydrolysis time. The exponential decrease in peak area of m/z 46 (NO_2^-) was used to quantify the observed hydrolysis rate constant, which is effectively the weighted average for the different structural isomers present in the solution, weighted by their relative concentrations. The m/z 62 (NO_3^-) fragment was used as a confirmation ion.

3 Results and Discussion

3.1 Organic nitrate yields

A primary objective for this study is quantitative measurements of organic nitrate yields from •OH reaction with ocimene, where the yields are defined as the concentration of $RONO_2$ produced ($\Delta RONO_2$ in ppb) relative to the concentration of BVOC consumed ($\Delta BVOC$ in ppb), i.e., $Y_{RONO2} = \Delta RONO_2/\Delta BVOC$ (Slade et al., 2017), corrected for losses of the organic nitrates. In our experiments, all peroxy radicals react with NO. Thus

$$RO_2 \quad + \quad NO \quad \rightarrow \quad RO \quad + \quad NO_2 \qquad\qquad (2a)$$

$$RO_2 \quad + \quad NO \quad \rightarrow \quad RONO_2 \qquad\qquad\qquad (2b)$$

$-d[ocimene]/dt = k_2[RO_2][NO]$, where $k_2 = k_{2a} + k_{2b}$, and $d[RONO_2]/dt = k_{2b}[RO_2][NO]$. Thus, $(d[RONO_2]/dt)/(-d[ocimene]/dt) = k_{2b}/k_2$. A plot of $\Delta[RONO_2]$ vs $-\Delta[ocimene]$ yields the RO_2-weighted average "branching ratio", k_{2b}/k_2 for the RO_2 radicals produced when •OH reacts with ocimene in the presence of O_2. We utilized the method of Kwok and Atkinson, 1995 to estimate the fraction of time that •OH adds to any of carbon #1, 2, 3, 4, 6, or 7, with numbers as shown here.
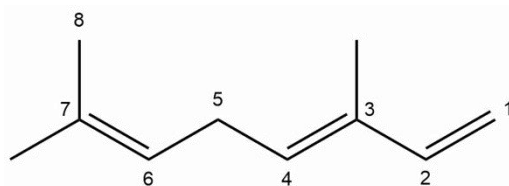
(E)-3,7-dimethylocta-1,3,6-triene

Because of the multiple double bonds, at which •OH can add, and because of the resonance structures of the multiple allylic radicals produced when •OH adds to C#s 1 or 4 (as shown for the most prevalent addition point, C4, in Figure 2), there are 10 possible main organic nitrate isomers, for each stereoisomer, i.e. the cis- or trans-ocimene, complicating the product analysis. Additional isomers may form from H-abstraction of the methyl groups, but these are of less significance than the isomers produced from •OH-addition to the double bond. The measured total hydroxynitrate, gas-, and particle-phase total organic nitrate yields under different RH are shown in Fig. 3. Yields are corrected for dilution in the chamber, loss to the chamber walls, loss during preconcentration, and hydroxynitrate consumption by reaction with •OH (Rindelaub et al., 2015; Slade et al., 2017). The error bars on individual points reflect the propagated

analytical uncertainties of the yields. The analytical uncertainty accounts for analytical errors associated

215 with all the steps involved in sample collection, extraction, and analysis, including denuder and filter extraction and collection efficiencies, uncertainty in the FTIR calibration when using a proxy for $-ONO_2$ quantitation, and, (for gas-phase hydroxynitrates), uncertainty in the CIMS sensitivity to the hydroxynitrate proxy. In Figure 3, we see that the observed total $RONO_2$ yield, and that for both gas- and aerosol-phases, and for the CIMS-determined hydroxy nitrates, are RH dependent, decreasing by $\sim\times2$

220 over the range studied (~3-70% RH). We interpret this as we did for the α-pinene case (Rindelaub et al., 2015), i.e. that hydroxy nitrates partition to the aerosol phase, where they are lost by hydrolysis. At higher RH, there will be more water associated with the particles, and the hydroxy nitrates are then more particle-soluble (Rindelaub et al., 2015). If we then extrapolate to 0% RH, the extent of particle-phase loss will be minimized, and thus the intercept represents the determined lower limit to the branching ratio. The

225 intercept for the total $RONO_2$ yield, as shown in Figure 3, is 33(±7)%, represented by the y-intercept of the black markers in Fig. 3a. In Figure 4, we present a summary of a range of observations of branching ratios for alkanes, alkenes, isoprene and the two terpenes for which we have determined the total yield (assumed RO_2-weighted average branching ratio). It is shown that the branching ratio for ocimene- and α-pinene- derived $RONO_2$ follows the trend observed for simple alkanes/alkenes, within the uncertainty

230 of the measurement (Arey et al., 2001; O'Brien et al., 1998; Rindelaub et al., 2015; Teng et al., 2015, 2017; Xiong et al., 2015).

We found that the first-generation hydroxy nitrates exist primarily in the gas phase (red markers in Fig. 3a), which is consistent with the low SOA yield, shown in Figure 5. Although the total $RONO_2$ yield of ocimene is greater than that for α-pinene oxidation, the particle phase organic nitrate yield is

235 much larger in the α-pinene case (Rindelaub et al., 2015). This is likely due to the fact that the SOA yield is much larger for α-pinene (34±12%; Rindelaub et al., 2016a), since, as discussed in the next section, ocimene oxidation produces smaller, more volatile, acyclic oxidation products. However, some of the low particle phase $RONO_2$ yield must occur because of the hydrolysis in the aerosol phase. The relatively low SOA yield can be attributed to the alkoxy radical decomposition products that produce the remaining 67%

240 of the first-generation oxidation products following the •OH-initiated pathway in the presence of NO_x, e.g. as shown producing methyl vinyl ketone and 2-methyl-2-pentenal, in Fig. 2. These decomposition

products are expected to be primarily C6- and smaller carbonyl compounds, of much higher volatility than the ocimene hydroxy nitrate. This occurs in the case of this linear tri-alkene, because scission of the C-C bond at the α-position to the alkoxy radical breaks the carbon chain into smaller chain carbonyl

245 compound products, as shown in Figure 2. As previously stated, the expected first-generation oxidation products (Fig. 2) are in the upper range of semi-volatile species, confirming their preferential presence in the gas phase (Donahue et al., 2011).

The CIMS-measured hydroxynitrate yields (green markers in Fig. 3a) are lower than the total gas-phase $RONO_2$ yield likely due to a lower CIMS sensitivity to the ocimene hydroxy nitrates than assumed,

250 using the α-pinene hydroxy nitrate standard used as a proxy. However, it is important to note that we expect all organic nitrates in this system to be hydroxy nitrates. In this regard, it is important that the CIMS-observed hydroxy nitrate concentration decayed to the same relative extent as for the FTIR-determined total, as shown in Figure 3. When the hydroxynitrate undergoes hydrolysis, the reaction proceeds likely via SN1 unimolecular nucleophilic substitution, as discussed in (Rindelaub et al., 2015).

255 The nitrooxy functional group serves as a leaving group and is replaced with a hydroxyl group, ultimately forming a diol. We calculated the vapor pressure of the diol produced from hydrolysis of Compound A in Figure 2, using SIMPOL (Pankow and Asher, 2008), and obtained 5.5×10^{-8} atm at 20ºC, which is identical to that calculated for compound A itself. However, it is likely that the Henry's Law constant for dissolution of the diol into water will increase (Shepson et al., 1996), effectively increasing the

260 partitioning into the aerosol phase.

3.2 SOA yields

Aerosol-mass-dependent secondary organic aerosol yields (Y_{SOA}) were calculated using the change in aerosol mass concentration (ΔM in µg m^{-3}) relative to the ocimene mass consumed ($\Delta BVOC$ in µg m^{-3}), i.e., $Y_{SOA} = \Delta M/\Delta BVOC$ (Slade et al., 2017). The aerosol mass concentration was derived

265 from the SMPS data, assuming spherical particles of 1.25 g cm^{-3} density (based on Ng et al., 2006), as shown in Fig. 1. The measured SOA yields as a function of aerosol mass and chamber RH are shown in Fig. 5a, where the error bars reflect the propagated analytical uncertainty of the yields when considering the wall loss and dilution correction. While there is an apparent increase in aerosol yield with increasing

humidity, it is not statistically significant (Figure 5a). We calculate from the data in Figure 5a that the

270   SOA yield from OH radical oxidation of ocimene is less than 1% for typical aerosol mass concentrations

in a moderately polluted forested environment, ~10 μg m^{-3}. These yields are lower than reported SOA

yields from α-pinene (34±12%), (Rindelaub et al., 2015). Again, we hypothesize that this is related to

structural differences of the alkoxy radicals, as shown in Figures 2 and 6, specifically that in the ocimene

case, cleavage of the α-carbon-carbon bond leads to two smaller radical fragments (Figure 2) and

275   ultimately more volatile smaller carbonyl compounds (Gaona-Colmán et al., 2018; Reissell, 2002). For

α-pinene, most of the products retain a C10 backbone (Rindelaub et al., 2016a), e.g. due to ring opening

reaction resulting from the α-carbon-carbon bond cleavage. To better understand the SOA yields, two-

product absorptive partitioning model fits of this study were compared to model fits and SOA yields of

similar acyclic, tri-olefinic monoterpenes, shown in Fig. 5b (Böge et al., 2013; Griffin et al., 1999;

280   Hoffmann et al., 1997). On average, the SOA yields in this study at all relative humidity values are less

but similar to that measured from ocimene photooxidation in a previous study, likely due to the absence

of O$_3$ in our study (Hoffmann et al., 1997). We find that the SOA yields for myrcene (also a linear triene)

were greater than those for ocimene (Böge et al., 2013). This is likely because of the two terminal double

bonds on myrcene that would result in a greater fraction of C$_9$ carbonyl compounds.

285   Low-volatility/water soluble organic nitrates can partition to the particle phase and contribute to

the SOA mass. The estimated vapor pressure (V$_P$) of the ocimene hydroxy nitrate is 5.6×10^{-8} atm at 20˚C

(Pankow and Asher, 2008), which is in the upper range of semi-volatile species, explaining the low

aerosol phase organic nitrate yields. This is in contrast to our experiments with alpha-pinene derived

hydroxy nitrates, where at low relative humidities, most RONO$_2$ was in the aerosol phase (Rindelaub et

290   al., 2015). The lower vapor pressure species likely lead to the greater aerosol yield (~×6) for α-pinene,

which in turn increased the partitioning of organic nitrates to the aerosol phase (Rindelaub et al., 2015).

It is now well known that aerosol liquid water can also influence the SOA growth. In the ambient

environment, as relative humidity increases (and as aerosol ages), the aerosol liquid water also increases

(Carlton and Turpin, 2013), driving uptake of water-soluble oxidized organic compounds (WSOC).

295   However, in the photochemical smog chamber used in this study, the extent of VOC oxidation is very

Atmospheric
Chemistry
and Physics
Discussions
Open Access
EGU

low (i.e. mostly primary products), and the resulting aerosols likely have relatively low O:C, resulting in a small correlation between relative humidity and aerosol yield, as shown in Figure 5.

The gas- and particle-phase extracts were analyzed using UHPLC-ToF-MS/MS to elucidate oxidation product structures. In Figure 7, the selected ion chromatograms (SIC) of expected oxidation

300 products from ESI negative mode are presented for both the filter (7a) and denuder (7b) extracts for experiment #6. As shown in the light blue trace in Figure 7, we do observe the dihydroxydinitrate, although the effective gas phase concentration could not be determined. As described above, we do correct for loss of the primary hydroxy nitrate by reaction with •OH. In the case of the dinitrate, such production would increase the effective measured organic nitrate yield. On the other hand, we also observe some of

305 the trihydroxynitrate, as shown in Figure 7, indicating partial hydrolysis of the dinitrate. In this case, the product is neutral in its impact on the measured organic nitrate yield, and as discussed below, given the hydrolysis rate constants, and the time scale of the experiments, it is likely that there is some hydrolysis of the primary organic nitrates to the corresponding diol, leading to the negative slope observed in Figure 3. We hypothesize that the smaller (C6 or C4) fragments produced during the oxidation were lost during

310 the solvent evaporation process, due to their high volatility.

3.3 Aqueous phase hydrolysis

The aqueous phase hydrolysis kinetics were further investigated by examining the decay of the gas- and particle-phase products using mass spectrometry. The RH dependence of the $RONO_2$ yields indicates acid-catalyzed hydrolysis. To date, there have only been hydrolysis rate constant determinations

315 for a few organic nitrates (Darer et al., 2011; Hu et al., 2011) and the α-pinene nitrate (Rindelaub et al., 2015), and a range of smaller hydroxy nitrates (Jacobs et al., 2014). Thus, we conducted measurements of the aqueous hydrolysis rate constants for the sum of the ocimene nitrates, via electrospray MS/MS, as a function of the solution pH. In Figure 8, we plot ln A_o/A_t vs t, in seconds, where zero is an arbitrary starting point for the pH-adjusted (buffered) samples. The resulting plots were linear as expected for a

320 first order exponential decay. The slope of each line is equal to the first-order hydrolysis rate constant. The symbols in this figure represent replicates for each pH, and each panel is a different pH, all on the same scale for each pH. As shown in Figure 8, the rate constants increase significantly, i.e. by ~×12, over

the range pH = 7.0 to pH = 2.5. These bulk rate constants represent those for the yield-average weighted organic nitrates produced.

325   In Figure 9, we plot our data for the ocimene nitrates, along with those for the α-pinene nitrate studied by Rindelaub et al., (2015). The equation for the best-fit line in Figure 9 is $\log_{10} k = -(0.24(pH) + 2.58)$, for ocimene. This shows that the natural lifetime against hydrolysis is 51 minutes at pH=4 and decreases to 11 minutes at pH=1. These are very short, compared to the lifetime of fine aerosol, i.e. ~1 week. Thus, we might expect that the aerosol phase concentration of such hydroxy nitrates might typically

330   be quite low, even though they have contributed significantly to aerosol mass, in the form of the diols. We also see that the hydrolysis lifetimes are very similar for the quite structurally different cyclic α-pinene nitrate and acyclic ocimene nitrates, i.e. 78 and 51 minutes, respectively, at pH=4. This implies that these values may be close to representative for a range of hydroxy nitrates. This rapid aqueous-phase hydrolysis can explain the difficulty to detect the presence of substantial aerosol phase organic nitrates

335   under ambient conditions (Ditto et al., 2020). As hydroxy nitrate production can represent an important fate for daytime oxidation of isoprene and terpenes in forest-impact environments, the uptake of these compounds into acidic aerosol followed by hydrolysis can represent an important mechanism for conversion of NO_x to HNO_3, as discussed in Romer Present et al., 2019 and Zare et al., 2018.

While the fate of the resulting diol in solution is unclear, there is a range of possible processes in

340   the aqueous phase, including OH radical attack and oligomerization. Further oxidation of these olefinic diols would likely result in fragmentation, which might then cause their release into the gas phase (Otto et al., 2017). Diols, and these olefinic diols, can also undergo oligomerization to form even lower volatility products which may have profound effects on the overall aerosol properties, such as viscosity and rate of diffusion (Glasius and Goldstein, 2016; Slade et al., 2019). The presence of oligomers from diols has

345   previously been identified, but molecular characterization is quite limited (Stropoli et al., 2019). Careful investigation of the structures of these oligomers is necessary. The nature of the oligomers must be determined to develop reliable predictive models of SOA formation (Budisulistiorini et al., 2017; Pye et al., 2013; Surratt et al., 2007).

4 Atmospheric Implications and Conclusions

350   The production of organic nitrates serves as an important sink for gas phase NO_x. The first generation organic nitrate products are relatively high vapor pressure and, for ocimene, are subject to further gas phase oxidative loss, to produce smaller, but more oxidized products (Bateman et al., 2011). While the main products of that oxidation will be hydroxy nitrooxy carbonyl compounds of lower carbon number, and thus perhaps higher vapor pressure, the yield of dihydroxy dinitrates will be significant. The

355   latter compounds will be much lower vapor pressure, e.g. that for Compound B shown in Figure 2, is 2.44×10^{-12} atm at 20 ˚C (Pankow and Asher, 2008), low enough that it should mostly undergo uptake into the aerosol phase, followed by hydrolysis to produce a 10-carbon tetrol and NO_3^-. However, the extent to which the gas phase oxidation of the primary product olefinic hydroxy nitrates re-releases NO_x needs to be studied from laboratory experiments with the pure compounds. The primary organic nitrates will

360   undergo hydrolysis in the particle phase, transforming from a hydroxynitrate to a diol. The nitrooxy group will be released as the nitrate ion, which can impact regional nitrogen cycling by either remaining in the particle phase (at certain pHs) or be released as gas phase nitric acid (at very high particle acidities). In either case, NO_x has been permanently removed from the system (Galbavy et al., 2007; Rindelaub et al., 2015; Suarez-Bertoa et al., 2012; Zafiriou and True, 1979; Zare et al., 2018; Romer Present et al., 2020).

365   Therefore, knowledge of the hydrolysis rate constants, especially for isoprene nitrates, is badly needed. The relatively large organic nitrate yield (33±7%) in combination with the rapid aqueous-phase hydrolysis both tend to make organic nitrate production an important sink for NO_x in terpene-impacted forest environments. In addition, the light dependent emission rate of ocimene suggests that in dense forest environments, like that of UMBS (Pratt et al., 2012), there could be steep vertical gradients in organic

370   nitrate concentrations between canopy and ground, exceeding that of the other terpene nitrates modelled in Schulze et al., 2017. It is thus necessary to further asses the organic nitrate yield values, hydrolysis rate constants, and major oxidation products for a range of terpenes to fully understand the impact of their oxidation on the fate and distribution of NOx.

   Further work should be done to examine the structural dependence of hydroxy nitrate hydrolysis

375   kinetics, e.g. the difference between β-hydroxy and δ-hydroxy nitrates. Previous work has determined thermodynamic stabilities of sterically different organic nitrates (primary, secondary, tertiary) based on

acid-catalyzed hydrolysis, where tertiary organic nitrates are less stable than primary or secondary organic nitrates at atmospherically-relevant pHs, suggesting potential differences in hydrolysis rates between β-hydroxy and δ-hydroxy nitrates (Hu et al., 2011). Differences between the hydrolysis rates of ocimene organic nitrates from NO_3- and OH-initiated oxidation should be explored, as significant differences in the hydrolysable fractions have been shown between organic nitrates formed from NO_3- and OH-initiated oxidation of both α- and β-pinene (Takeuchi and Ng, 2019), and daytime NO_3 concentrations can be relevant in forests like that of UMBS (Pratt et al., 2012; Schulze et al., 2017). It is necessary to understand the SOA components produced during this oxidation to better predict aqueous phase processing. Further work on the condensed phase chemistry of alcohols and olefinic oxygenated compounds in the aerosol phase is necessary. These results suggest that ocimene hydroxy organic nitrates may be an important sink for gas phase NO_x in forest environments.

6 Acknowledgement

References

Arey, J., Aschmann, S. M., Kwok, E. S. C. and Atkinson, R.: Alkyl Nitrate, Hydroxyalkyl Nitrate, and Hydroxycarbonyl Formation from the NO $_x$ −Air Photooxidations of C $_5$ −C $_8$ n -Alkanes, J. Phys. Chem. A, 105(6), 1020–1027, doi:10.1021/jp003292z, 2001.

Atkinson, R. and Arey, J.: Gas-phase tropospheric chemistry of biogenic volatile organic compounds: a review, Atmos. Environ., 37, 197–219, doi:10.1016/S1352-2310(03)00391-1, 2003.

Atkinson, R., Baulch, D. L., Cox, R. A., Crowley, J. N., Hampson, R. F., Hynes, R. G., Jenkin, M. E., Rossi, M. J., Troe, J. and IUPAC Subcommittee: Evaluated kinetic and photochemical data for atmospheric chemistry: Volume II - gas phase reactions of organic species, Atmospheric Chem. Phys., 6(11), 3625–4055, doi:10.5194/acp-6-3625-2006, 2006.

Bateman, A. P., Nizkorodov, S. A., Laskin, J. and Laskin, A.: Photolytic processing of secondary organic aerosols dissolved in cloud droplets, Phys. Chem. Chem. Phys., 13(26), 12199, doi:10.1039/c1cp20526a, 2011.

Bean, J. K. and Hildebrandt Ruiz, L.: Gas–particle partitioning and hydrolysis of organic nitrates formed from the oxidation of α -pinene in environmental chamber experiments, Atmospheric Chem. Phys., 16(4), 2175–2184, doi:10.5194/acp-16-2175-2016, 2016.

Biesenthal, T. A., Wu, Q., Shepson, P. B., Wiebe, H. A., Anlauf, K. G. and Mackay, G. I.: A study of relationships between isoprene, its oxidation products, and ozone, in the Lower Fraser Valley, BC, Atmos. Environ., 31(14), 2049–2058, doi:10.1016/S1352-2310(96)00318-4, 1997.

Böge, O., Mutzel, A., Iinuma, Y., Yli-Pirilä, P., Kahnt, A., Joutsensaari, J. and Herrmann, H.: Gas-phase products and secondary organic aerosol formation from the ozonolysis and photooxidation of myrcene, Atmos. Environ., 79, 553–560, doi:10.1016/j.atmosenv.2013.07.034, 2013.

Boyd, C. M., Sanchez, J., Xu, L., Eugene, A. J., Nah, T., Tuet, W. Y., Guzman, M. I. and Ng, N. L.: Secondary organic aerosol formation from the β-pinene+NO $_3$ system: effect of humidity and peroxy radical fate, Atmospheric Chem. Phys., 15(13), 7497–7522, doi:10.5194/acp-15-7497-2015, 2015.

Browne, E. C. and Cohen, R. C.: Effects of biogenic nitrate chemistry on the NOx lifetime in remote continental regions, Atmospheric Chem. Phys., 12(24), 11917–11932, doi:10.5194/acp-12-11917-2012, 2012.

Budisulistiorini, S. H., Nenes, A., Carlton, A. G., Surratt, J. D., McNeill, V. F. and Pye, H. O. T.: Simulating Aqueous-Phase Isoprene-Epoxydiol (IEPOX) Secondary Organic Aerosol Production During the 2013 Southern Oxidant and Aerosol Study (SOAS), Environ. Sci. Technol., 51(9), 5026–5034, doi:10.1021/acs.est.6b05750, 2017.

Capouet, M., Peeters, J., Nozi`ere, B. and Müller, J.-F.: Alpha-pinene oxidation by OH: simulations of laboratory experiments, Atmospheric Chem. Phys., 4(9/10), 2285–2311, doi:10.5194/acp-4-2285-2004, 2004.

435 Carlton, A. G. and Turpin, B. J.: Particle partitioning potential of organic compounds is highest in the Eastern US and driven by anthropogenic water, Atmospheric Chem. Phys., 13(20), 10203–10214, doi:10.5194/acp-13-10203-2013, 2013.

Chen, X., Hulbert, D. and Shepson, P. B.: Measurement of the organic nitrate yield from OH reaction with isoprene, J. Geophys. Res. Atmospheres, 103(D19), 25563–25568, doi:10.1029/98JD01483, 1998.

440 Darer, A. I., Cole-Filipiak, N. C., O'Connor, A. E. and Elrod, M. J.: Formation and Stability of Atmospherically Relevant Isoprene-Derived Organosulfates and Organonitrates, Environ. Sci. Technol., 45(5), 1895–1902, doi:10.1021/es103797z, 2011.

Ditto, J. C., Joo, T., Slade, J. H., Shepson, P. B., Ng, N. L. and Gentner, D. R.: Nontargeted Tandem Mass Spectrometry Analysis Reveals Diversity and Variability in Aerosol Functional Groups across Multiple 445 Sites, Seasons, and Times of Day, Environ. Sci. Technol. Lett., 7(2), 60–69, doi:10.1021/acs.estlett.9b00702, 2020.

Donahue, N. M., Epstein, S. A., Pandis, S. N. and Robinson, A. L.: A two-dimensional volatility basis set: 1. organic-aerosol mixing thermodynamics, Atmospheric Chem. Phys., 11(7), 3303–3318, doi:10.5194/acp-11-3303-2011, 2011.

450 Fry, J. L., Kiendler-Scharr, A., Rollins, A. W., Wooldridge, P. J., Brown, S. S., Fuchs, H., Dube, W., Mensah, A., dal Maso, M., Tillmann, R., Dorn, H. P., Brauers, T. and Cohen, R. C.: Organic nitrate and secondary organic aerosol yield from NO3 oxidation of beta-pinene evaluated using a gas-phase kinetics/aerosol partitioning model, Atmospheric Chem. Phys., 9(4), 1431–1449, 2009.

Fry, J. L., Draper, D. C., Barsanti, K. C., Smith, J. N., Ortega, J., Winkler, P. M., Lawler, M. J., Brown, 455 S. S., Edwards, P. M., Cohen, R. C. and Lee, L.: Secondary Organic Aerosol Formation and Organic Nitrate Yield from NO$_3$ Oxidation of Biogenic Hydrocarbons, Environ. Sci. Technol., 48(20), 11944–11953, doi:10.1021/es502204x, 2014.

Galbavy, E. S., Anastasio, C., Lefer, B. and Hall, S.: Light penetration in the snowpack at Summit, Greenland: Part 2 Nitrate photolysis, Atmos. Environ., 41(24), 5091–5100, 460 doi:10.1016/j.atmosenv.2006.01.066, 2007.

Gaona-Colmán, E., Blanco, M. B., Barnes, I., Wiesen, P. and Teruel, M. A.: Atmospheric sink of β-ocimene and camphene initiated by Cl atoms: kinetics and products at NO$_x$ free-air, RSC Adv., 8(48), 27054–27063, doi:10.1039/C8RA04931A, 2018.

Glasius, M. and Goldstein, A. H.: Recent Discoveries and Future Challenges in Atmospheric Organic
465 Chemistry, Environ. Sci. Technol., 50(6), 2754–2764, doi:10.1021/acs.est.5b05105, 2016.

Goldstein, A. H. and Galbally, I. E.: Known and Unexplored Organic Constituents in the Earth's
Atmosphere, Environ. Sci. Technol., 41(5), 1514–1521, doi:10.1021/es072476p, 2007.

Griffin, R. J., Cocker, D. R., Seinfeld, J. H. and Dabdub, D.: Estimate of global atmospheric organic
aerosol from oxidation of biogenic hydrocarbons, Geophys. Res. Lett., 26(17), 2721–2724,
470 doi:10.1029/1999GL900476, 1999.

Guenther, A., Hewitt, C. N., Erickson, D., Fall, R., Geron, C., Graedel, T., Harley, P., Klinger, L., Lerdau,
M., Mckay, W. A., Pierce, T., Scholes, B., Steinbrecher, R., Tallamraju, R., Taylor, J. and Zimmerman,
P.: A global model of natural volatile organic compound emissions, J. Geophys. Res., 100(D5), 8873,
doi:10.1029/94JD02950, 1995.

475 Guenther, A. B., Jiang, X., Heald, C. L., Sakulyanontvittaya, T., Duhl, T., Emmons, L. K. and Wang, X.:
The Model of Emissions of Gases and Aerosols from Nature version 2.1 (MEGAN2.1): an extended and
updated framework for modeling biogenic emissions, Geosci Model Dev, 5(6), 1471–1492,
doi:10.5194/gmd-5-1471-2012, 2012.

Hallquist, M., Wenger, J. C., Baltensperger, U., Rudich, Y., Simpson, D., Claeys, M., Dommen, J.,
480 Donahue, N. M., George, C., Goldstein, A. H., Hamilton, J. F., Herrmann, H., Hoffmann, T., Iinuma, Y.,
Jang, M., Jenkin, M. E., Jimenez, J. L., Kiendler-Scharr, A., Maenhaut, W., McFiggans, G., Mentel, Th.
F., Monod, A., Prévôt, A. S. H., Seinfeld, J. H., Surratt, J. D., Szmigielski, R. and Wildt, J.: The formation,
properties and impact of secondary organic aerosol: current and emerging issues, Atmospheric Chem.
Phys., 9(14), 5155–5236, doi:10.5194/acp-9-5155-2009, 2009.

485 Hatakeyama, S., Izumi, K., Fukuyama, T., Akimoto, H. and Washida, N.: Reactions of OH with α-pinene
and β-pinene in air: Estimate of global CO production from the atmospheric oxidation of terpenes, J.
Geophys. Res., 96(D1), 947, doi:10.1029/90JD02341, 1991.

Hoffmann, T., Odum, J. R., Bowman, F., Collins, D., Klockow, D., Flagan, R. C. and Seinfeld, J. H.: [No
title found], J. Atmospheric Chem., 26(2), 189–222, doi:10.1023/A:1005734301837, 1997.

490 Hu, K. S., Darer, A. I. and Elrod, M. J.: Thermodynamics and kinetics of the hydrolysis of atmospherically
relevant organonitrates and organosulfates, Atmospheric Chem. Phys., 11(16), 8307–8320,
doi:10.5194/acp-11-8307-2011, 2011.

Isaksen, I. S. A., Granier, C., Myhre, G., Berntsen, T. K., Dalsøren, S. B., Gauss, M., Klimont, Z.,
Benestad, R., Bousquet, P., Collins, W., Cox, T., Eyring, V., Fowler, D., Fuzzi, S., Jöckel, P., Laj, P.,
495 Lohmann, U., Maione, M., Monks, P., Prevot, A. S. H., Raes, F., Richter, A., Rognerud, B., Schulz, M.,
Shindell, D., Stevenson, D. S., Storelvmo, T., Wang, W.-C., van Weele, M., Wild, M. and Wuebbles, D.:

Atmospheric composition change: Climate–Chemistry interactions, Atmos. Environ., 43(33), 5138–5192, doi:10.1016/j.atmosenv.2009.08.003, 2009.

Jacobs, M. I., Burke, W. J. and Elrod, M. J.: Kinetics of the reactions of isoprene-derived hydroxynitrates: gas phase epoxide formation and solution phase hydrolysis, Atmospheric Chem. Phys., 14(17), 8933–8946, doi:10.5194/acp-14-8933-2014, 2014.

Kwok, E. and Atkinson, R.: Estimation of hydroxyl radical reaction rate constants for gas-phase organic compounds using a structure-reactivity relationship: An update, Atmos. Environ., 29(14), 1685–1695, doi:10.1016/1352-2310(95)00069-B, 1995.

Lee, A., Goldstein, A. H., Kroll, J. H., Ng, N. L., Varutbangkul, V., Flagan, R. C. and Seinfeld, J. H.: Gas-phase products and secondary aerosol yields from the photooxidation of 16 different terpenes, J. Geophys. Res., 111(D17), doi:10.1029/2006JD007050, 2006.

Lee, B. H., Mohr, C., Lopez-Hilfiker, F. D., Lutz, A., Hallquist, M., Lee, L., Romer, P., Cohen, R. C., Iyer, S., Kurtén, T., Hu, W., Day, D. A., Campuzano-Jost, P., Jimenez, J. L., Xu, L., Ng, N. L., Guo, H., Weber, R. J., Wild, R. J., Brown, S. S., Koss, A., de Gouw, J., Olson, K., Goldstein, A. H., Seco, R., Kim, S., McAvey, K., Shepson, P. B., Starn, T., Baumann, K., Edgerton, E. S., Liu, J., Shilling, J. E., Miller, D. O., Brune, W., Schobesberger, S., D'Ambro, E. L. and Thornton, J. A.: Highly functionalized organic nitrates in the southeast United States: Contribution to secondary organic aerosol and reactive nitrogen budgets, Proc. Natl. Acad. Sci., 113(6), 1516–1521, doi:10.1073/pnas.1508108113, 2016.

Liu, S., Shilling, J. E., Song, C., Hiranuma, N., Zaveri, R. A. and Russell, L. M.: Hydrolysis of Organonitrate Functional Groups in Aerosol Particles, Aerosol Sci. Technol., 46(12), 1359–1369, doi:10.1080/02786826.2012.716175, 2012.

Lockwood, A. L., Shepson, P. B., Fiddler, M. N. and Alaghmand, M.: Isoprene nitrates: preparation, separation, identification, yields, and atmospheric chemistry, Atmospheric Chem. Phys., 10(13), 6169–6178, doi:10.5194/acp-10-6169-2010, 2010.

Monks, P. S., Granier, C., Fuzzi, S., Stohl, A., Williams, M. L., Akimoto, H., Amann, M., Baklanov, A., Baltensperger, U., Bey, I., Blake, N., Blake, R. S., Carslaw, K., Cooper, O. R., Dentener, F., Fowler, D., Fragkou, E., Frost, G. J., Generoso, S., Ginoux, P., Grewe, V., Guenther, A., Hansson, H. C., Henne, S., Hjorth, J., Hofzumahaus, A., Huntrieser, H., Isaksen, I. S. A., Jenkin, M. E., Kaiser, J., Kanakidou, M., Klimont, Z., Kulmala, M., Laj, P., Lawrence, M. G., Lee, J. D., Liousse, C., Maione, M., McFiggans, G., Metzger, A., Mieville, A., Moussiopoulos, N., Orlando, J. J., O'Dowd, C. D., Palmer, P. I., Parrish, D. D., Petzold, A., Platt, U., Pöschl, U., Prévôt, A. S. H., Reeves, C. E., Reimann, S., Rudich, Y., Sellegri, K., Steinbrecher, R., Simpson, D., ten Brink, H., Theloke, J., van der Werf, G. R., Vautard, R., Vestreng, V., Vlachokostas, Ch. and von Glasow, R.: Atmospheric composition change – global and regional air quality, Atmos. Environ., 43(33), 5268–5350, doi:10.1016/j.atmosenv.2009.08.021, 2009.

Ng, N. L., Kroll, J. H., Keywood, M. D., Bahreini, R., Varutbangkul, V., Flagan, R. C., Seinfeld, J. H., Lee, A. and Goldstein, A. H.: Contribution of First- versus Second-Generation Products to Secondary Organic Aerosols Formed in the Oxidation of Biogenic Hydrocarbons, Environ. Sci. Technol., 40(7), 2283–2297, doi:10.1021/es052269u, 2006.

535   Nielsen, T., Egeløv, A. H., Granby, K. and Skov, H.: Observations on particulate organic nitrates and unidentified components of NOy, Atmos. Environ., 29(15), 1757–1769, doi:10.1016/1352-2310(95)00098-J, 1995.

O'Brien, J. M., Czuba, E., Hastie, D. R., Francisco, Joseph. S. and Shepson, P. B.: Determination of the Hydroxy Nitrate Yields from the Reaction of $C_2 - C_6$ Alkenes with OH in the Presence of NO, J. Phys.
540   Chem. A, 102(45), 8903–8908, doi:10.1021/jp982320z, 1998.

Otto, T., Stieger, B., Mettke, P. and Herrmann, H.: Tropospheric Aqueous-Phase Oxidation of Isoprene-Derived Dihydroxycarbonyl Compounds, J. Phys. Chem. A, 121(34), 6460–6470, doi:10.1021/acs.jpca.7b05879, 2017.

Pankow, J. F. and Asher, W. E.: SIMPOL.1: a simple group contribution method for predicting vapor
545   pressures and enthalpies of vaporization of multifunctional organic compounds, Atmospheric Chem. Phys., 8(10), 2773–2796, doi:10.5194/acp-8-2773-2008, 2008.

Perraud, V., Bruns, E. A., Ezell, M. J., Johnson, S. N., Yu, Y., Alexander, M. L., Zelenyuk, A., Imre, D., Chang, W. L., Dabdub, D., Pankow, J. F. and Finlayson-Pitts, B. J.: Nonequilibrium atmospheric secondary organic aerosol formation and growth, Proc. Natl. Acad. Sci., 109(8), 2836–2841,
550   doi:10.1073/pnas.1119909109, 2012.

Perring, A. E., Pusede, S. E. and Cohen, R. C.: An Observational Perspective on the Atmospheric Impacts of Alkyl and Multifunctional Nitrates on Ozone and Secondary Organic Aerosol, Chem. Rev., 113(8), 5848–5870, doi:10.1021/cr300520x, 2013.

Possanzini, M., Palo, V. D. and Cecinato, A.: Sources and photodecomposition of formaldehyde and
555   acetaldehyde in Rome ambient air, Atmos. Environ., 36(19), 3195–3201, doi:10.1016/S1352-2310(02)00192-9, 2002.

Pratt, K. A., Mielke, L. H., Shepson, P. B., Bryan, A. M., Steiner, A. L., Ortega, J., Daly, R., Helmig, D., Vogel, C. S., Griffith, S., Dusanter, S., Stevens, P. S. and Alaghmand, M.: Contributions of individual reactive biogenic volatile organic compounds to organic nitrates above a mixed forest, Atmospheric
560   Chem. Phys., 12(21), 10125–10143, doi:10.5194/acp-12-10125-2012, 2012.

Pusede, S. E., Steiner, A. L. and Cohen, R. C.: Temperature and Recent Trends in the Chemistry of Continental Surface Ozone, Chem. Rev., 115(10), 3898–3918, doi:10.1021/cr5006815, 2015.

Pye, H. O. T., Pinder, R. W., Piletic, I. R., Xie, Y., Capps, S. L., Lin, Y.-H., Surratt, J. D., Zhang, Z., Gold, A., Luecken, D. J., Hutzell, W. T., Jaoui, M., Offenberg, J. H., Kleindienst, T. E., Lewandowski, M. and Edney, E. O.: Epoxide Pathways Improve Model Predictions of Isoprene Markers and Reveal Key Role of Acidity in Aerosol Formation, Environ. Sci. Technol., 47(19), 11056–11064, doi:10.1021/es402106h, 2013.

Pye, H. O. T., Luecken, D. J., Xu, L., Boyd, C. M., Ng, N. L., Baker, K. R., Ayres, B. R., Bash, J. O., Baumann, K., Carter, W. P. L., Edgerton, E., Fry, J. L., Hutzell, W. T., Schwede, D. B. and Shepson, P. B.: Modeling the Current and Future Roles of Particulate Organic Nitrates in the Southeastern United States, Environ. Sci. Technol., 49(24), 14195–14203, doi:10.1021/acs.est.5b03738, 2015.

Reissell, A.: Products of the OH radical- and O$_3$-initiated reactions of myrcene and ocimene, J. Geophys. Res., 107(D12), 4138, doi:10.1029/2001JD001234, 2002.

Rindelaub, J. D., McAvey, K. M. and Shepson, P. B.: The photochemical production of organic nitrates from α-pinene and loss via acid-dependent particle phase hydrolysis, Atmos. Environ., 100, 193–201, doi:10.1016/j.atmosenv.2014.11.010, 2015.

Rindelaub, J. D., Wiley, J. S., Cooper, B. R. and Shepson, P. B.: Chemical characterization of α-pinene secondary organic aerosol constituents using gas chromatography, liquid chromatography, and paper spray-based mass spectrometry techniques: Characterization of α-pinene SOA constituents, Rapid Commun. Mass Spectrom., 30(13), 1627–1638, doi:10.1002/rcm.7602, 2016a.

Rindelaub, J. D., Borca, C. H., Hostetler, M. A., Slade, J. H., Lipton, M. A., Slipchenko, L. V. and Shepson, P. B.: The acid-catalyzed hydrolysis of an α-pinene-derived organic nitrate: kinetics, products, reaction mechanisms, and atmospheric impact, Atmospheric Chem. Phys., 16(23), 15425–15432, doi:10.5194/acp-16-15425-2016, 2016b.

Rollins, A. W., Browne, E. C., Min, K.-E., Pusede, S. E., Wooldridge, P. J., Gentner, D. R., Goldstein, A. H., Liu, S., Day, D. A., Russell, L. M. and Cohen, R. C.: Evidence for NOx Control over Nighttime SOA Formation, Science, 337(6099), 1210–1212, doi:10.1126/science.1221520, 2012.

Rollins, A. W., Pusede, S., Wooldridge, P., Min, K.-E., Gentner, D. R., Goldstein, A. H., Liu, S., Day, D. A., Russell, L. M., Rubitschun, C. L., Surratt, J. D. and Cohen, R. C.: Gas/particle partitioning of total alkyl nitrates observed with TD-LIF in Bakersfield: RONO2 PHASE PARTITIONING, J. Geophys. Res. Atmospheres, 118(12), 6651–6662, doi:10.1002/jgrd.50522, 2013.

Romer, P. S., Duffey, K. C., Wooldridge, P. J., Allen, H. M., Ayres, B. R., Brown, S. S., Brune, W. H., Crounse, J. D., De Gouw, J. and Draper, D. C.: The lifetime of nitrogen oxides in an isoprene-dominated forest, Atmospheric Chem. Phys., 16(12), 7623–7637, 2016.

595   Romer Present, P. S., Zare, A. and Cohen, R. C.: The changing role of organic nitrates in the removal and transport of NOx, preprint, Gases/Field Measurements/Troposphere/Chemistry (chemical composition and reactions)., 2019.

Schulze, B. C., Wallace, H. W., Flynn, J. H., Lefer, B. L., Erickson, M. H., Jobson, B. T., Dusanter, S., Griffith, S. M., Hansen, R. F., Stevens, P. S., VanReken, T. and Griffin, R. J.: Differences in BVOC
600   oxidation and SOA formation above and below the forest canopy, Atmospheric Chem. Phys., 17(3), 1805–1828, doi:10.5194/acp-17-1805-2017, 2017.

Shepson, P. B., Mackay, E. and Muthuramu, K.: Henry's Law Constants and Removal Processes for Several Atmospheric β-Hydroxy Alkyl Nitrates, Environ. Sci. Technol., 30(12), 3618–3623, doi:10.1021/es960538y, 1996.

605   Slade, J. H., de Perre, C., Lee, L. and Shepson, P. B.: Nitrate radical oxidation of γ-terpinene: hydroxy nitrate, total organic nitrate, and secondary organic aerosol yields, Atmospheric Chem. Phys., 17(14), 8635–8650, doi:10.5194/acp-17-8635-2017, 2017.

Slade, J. H., Ault, A. P., Bui, A. T., Ditto, J. C., Lei, Z., Bondy, A. L., Olson, N. E., Cook, R. D., Desrochers, S. J., Harvey, R. M., Erickson, M. H., Wallace, H. W., Alvarez, S. L., Flynn, J. H., Boor, B.
610   E., Petrucci, G. A., Gentner, D. R., Griffin, R. J. and Shepson, P. B.: Bouncier Particles at Night: Biogenic Secondary Organic Aerosol Chemistry and Sulfate Drive Diel Variations in the Aerosol Phase in a Mixed Forest, Environ. Sci. Technol., 53(9), 4977–4987, doi:10.1021/acs.est.8b07319, 2019.

Stropoli, S. J., Miner, C. R., Hill, D. R. and Elrod, M. J.: Assessing Potential Oligomerization Reaction Mechanisms of Isoprene Epoxydiols on Secondary Organic Aerosol, Environ. Sci. Technol., 53(1), 176–
615   184, doi:10.1021/acs.est.8b05247, 2019.

Suarez-Bertoa, R., Picquet-Varrault, B., Tamas, W., Pangui, E. and Doussin, J.-F.: Atmospheric Fate of a Series of Carbonyl Nitrates: Photolysis Frequencies and OH-Oxidation Rate Constants, Environ. Sci. Technol., 46(22), 12502–12509, doi:10.1021/es302613x, 2012.

Surratt, J. D., Kroll, J. H., Kleindienst, T. E., Edney, E. O., Claeys, M., Sorooshian, A., Ng, N. L.,
620   Offenberg, J. H., Lewandowski, M., Jaoui, M., Flagan, R. C. and Seinfeld, J. H.: Evidence for Organosulfates in Secondary Organic Aerosol, Environ. Sci. Technol., 41(2), 517–527, doi:10.1021/es062081q, 2007.

Surratt, J. D., Gómez-González, Y., Chan, A. W. H., Vermeylen, R., Shahgholi, M., Kleindienst, T. E., Edney, E. O., Offenberg, J. H., Lewandowski, M., Jaoui, M., Maenhaut, W., Claeys, M., Flagan, R. C.
625   and Seinfeld, J. H.: Organosulfate Formation in Biogenic Secondary Organic Aerosol, J. Phys. Chem. A, 112(36), 8345–8378, doi:10.1021/jp802310p, 2008.

Takeuchi, M. and Ng, N. L.: Chemical composition and hydrolysis of organic nitrate aerosol formed from hydroxyl and nitrate radical oxidation of α -pinene and β -pinene, Atmospheric Chem. Phys., 19(19), 12749–12766, doi:10.5194/acp-19-12749-2019, 2019.

630 Teng, A. P., Crounse, J. D., Lee, L., St. Clair, J. M., Cohen, R. C. and Wennberg, P. O.: Hydroxy nitrate production in the OH-initiated oxidation of alkenes, Atmospheric Chem. Phys., 15(8), 4297–4316, doi:10.5194/acp-15-4297-2015, 2015.

Teng, A. P., Crounse, J. D. and Wennberg, P. O.: Isoprene Peroxy Radical Dynamics, J. Am. Chem. Soc., 139(15), 5367–5377, doi:10.1021/jacs.6b12838, 2017.

635 Tsigaridis, K. and Kanakidou, M.: Secondary organic aerosol importance in the future atmosphere, Atmos. Environ., 41(22), 4682–4692, doi:10.1016/j.atmosenv.2007.03.045, 2007.

Walker, R. D. and Hawkins, J. E.: The Ultraviolet Absorption Spectra of Some Terpene Hydrocarbons, J. Am. Chem. Soc., 74(16), 4209–4210, doi:10.1021/ja01136a512, 1952.

Xiong, F., McAvey, K. M., Pratt, K. A., Groff, C. J., Hostetler, M. A., Lipton, M. A., Starn, T. K., Seeley, 640 J. V., Bertman, S. B., Teng, A. P., Crounse, J. D., Nguyen, T. B., Wennberg, P. O., Misztal, P. K., Goldstein, A. H., Guenther, A. B., Koss, A. R., Olson, K. F., de Gouw, J. A., Baumann, K., Edgerton, E. S., Feiner, P. A., Zhang, L., Miller, D. O., Brune, W. H. and Shepson, P. B.: Observation of isoprene hydroxynitrates in the southeastern United States and implications for the fate of NOx, Atmos Chem Phys, 15(19), 11257–11272, doi:10.5194/acp-15-11257-2015, 2015.

645 Xiong, F., Borca, C. H., Slipchenko, L. V. and Shepson, P. B.: Photochemical degradation of isoprene-derived 4,1-nitrooxy enal, Atmospheric Chem. Phys., 16(9), 5595–5610, doi:10.5194/acp-16-5595-2016, 2016.

Zafiriou, O. C. and True, M. B.: Nitrate photolysis in seawater by sunlight, Mar. Chem., 8(1), 33–42, doi:10.1016/0304-4203(79)90030-6, 1979.

650 Zare, A., Romer, P. S., Nguyen, T., Keutsch, F. N., Skog, K. and Cohen, R. C.: A comprehensive organic nitrate chemistry: insights into the lifetime of atmospheric organic nitrates, Atmospheric Chem. Phys., 18(20), 15419–15436, doi:10.5194/acp-18-15419-2018, 2018.
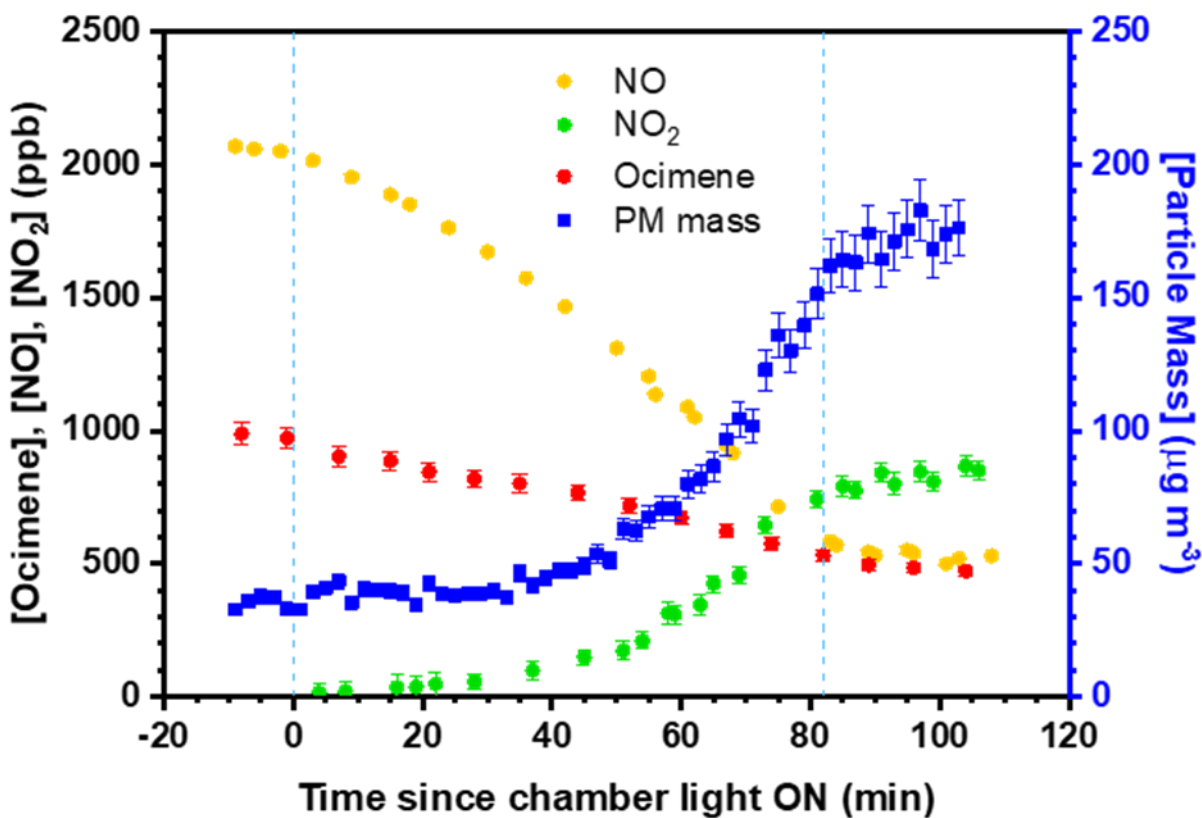
Figure 1: Time series of ocimene oxidation and particle formation for experiment #6. The error bars represent the propagated analytical uncertainty and blue dashed lines represent the time of UV light irradiation. (PM = particulate matter).

655
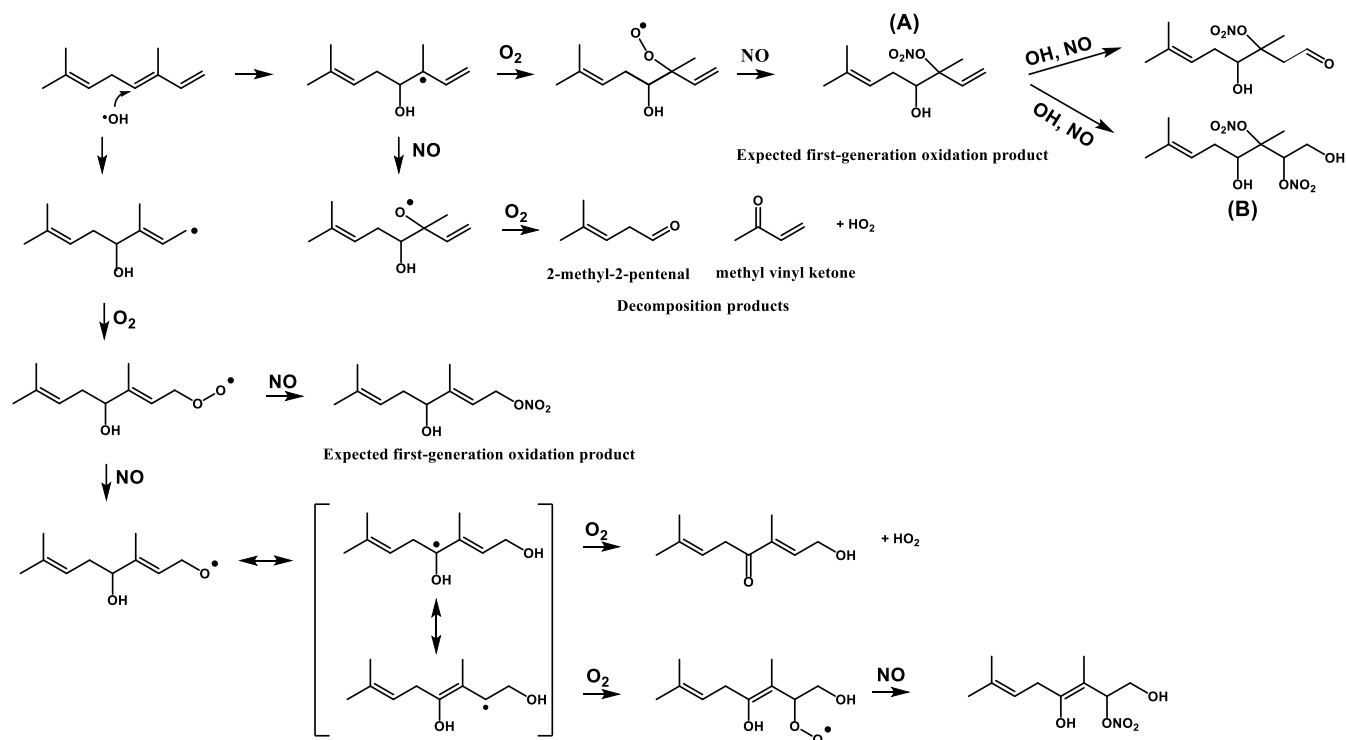
Figure 2: Example reaction pathways of the •OH-initiated oxidation of β-ocimene in the presence of NO$_x$.
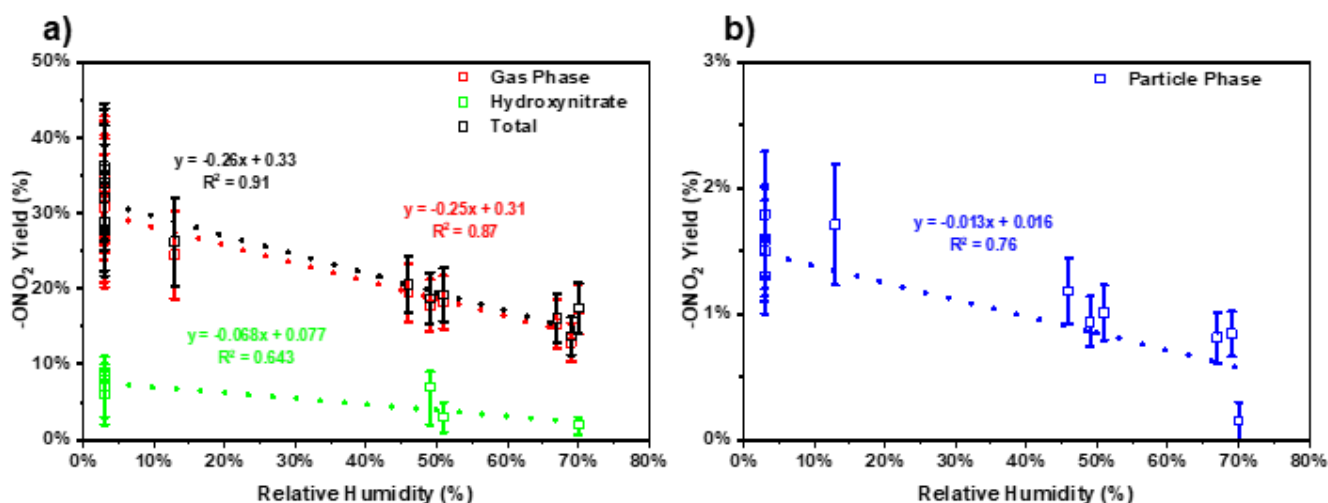
Figure 3: a) Wall-loss and dilution-corrected, total gas-phase organic nitrate (-ONO2), total (both gas- and particle-phase) organic nitrate (quantified by FTIR) and hydroxynitrate (quantified by CIMS) yield at

different RH. b) Wall-loss and dilution-corrected, total particle-phase organic nitrate yield at different RH. Error bars represent the propagated analytical uncertainty of the yields.
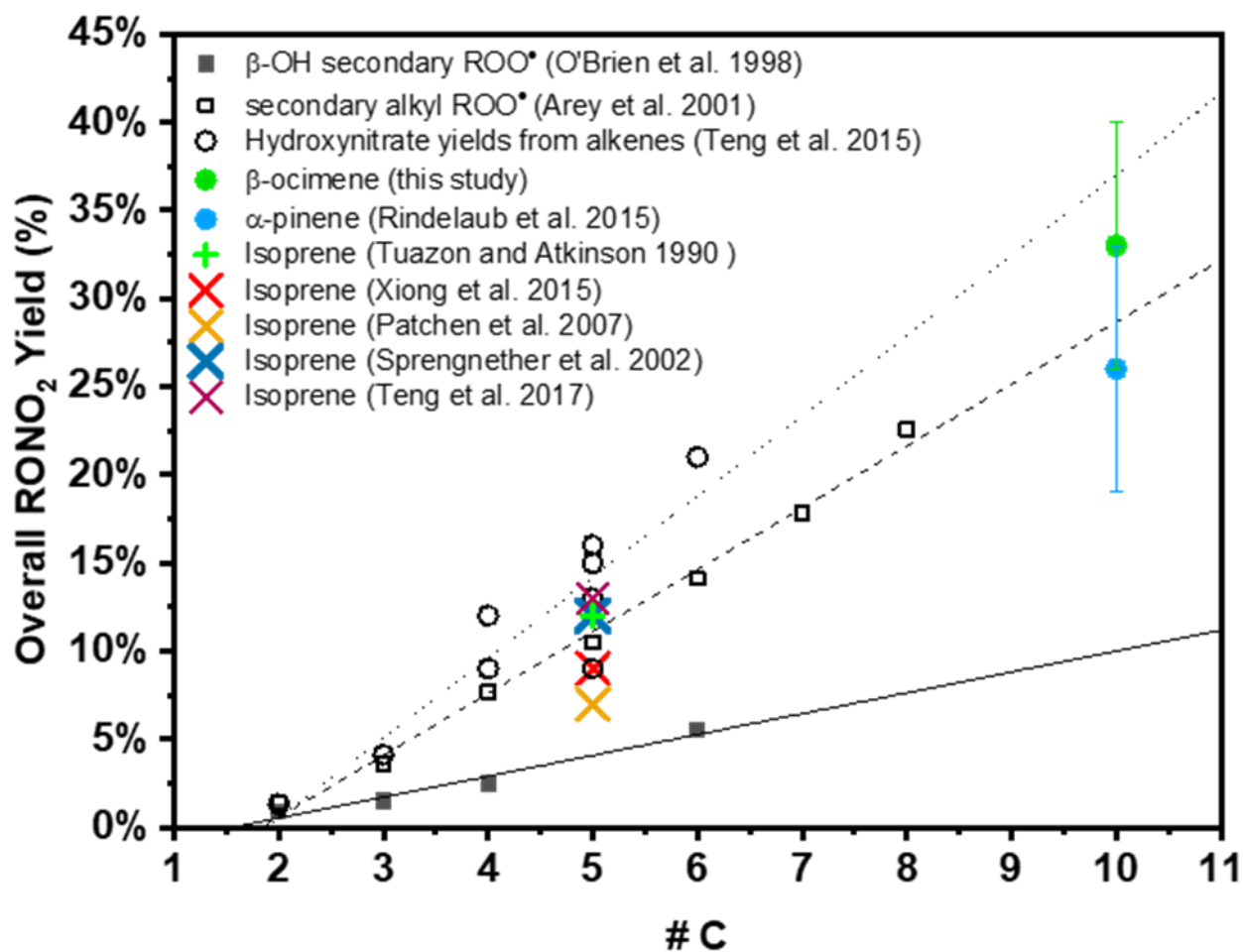
Figure 4: Atmospheric pressure branching ratio vs size for alkyl peroxy radicals.

670
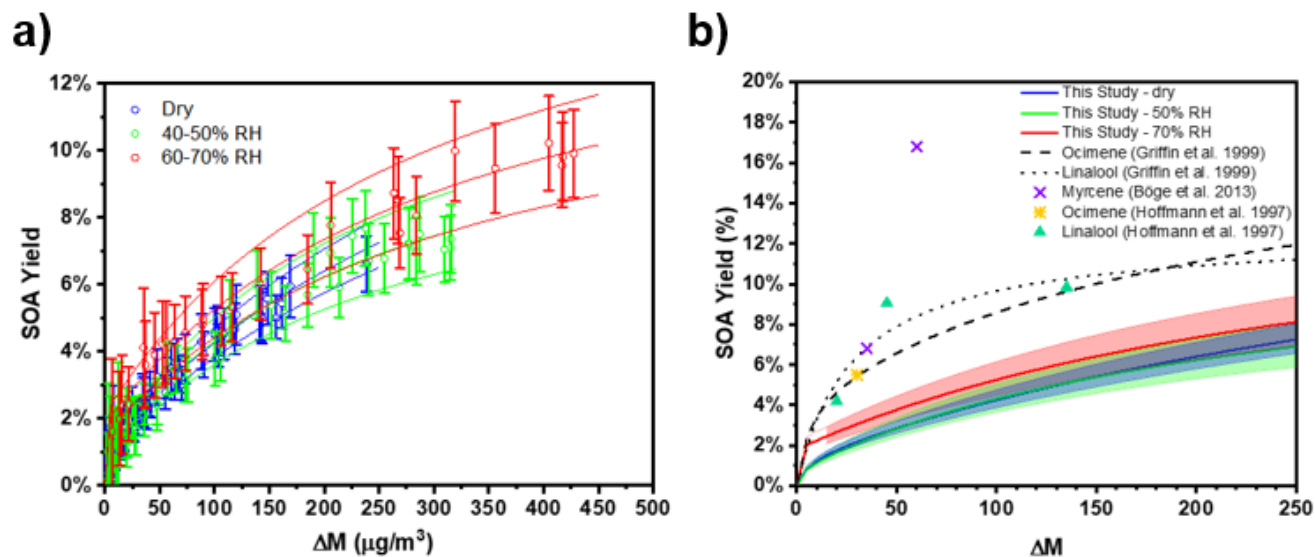
Figure 5: a) Change in PM mass concentration (ΔM) and secondary organic aerosol yields for seeded experiments under different RH conditions. The solid lines indicate the two-product absorptive partitioning model fit and the dashed lines represent the 95% confidence intervals of the fitting function. b) Two-product absorptive partitioning model fits of this study vs model fits and SOA yield % reported in the literature for the acyclic triolefinic and oxygenated terpenes. The shaded regions represent the 95% confidence intervals of the fitting function.
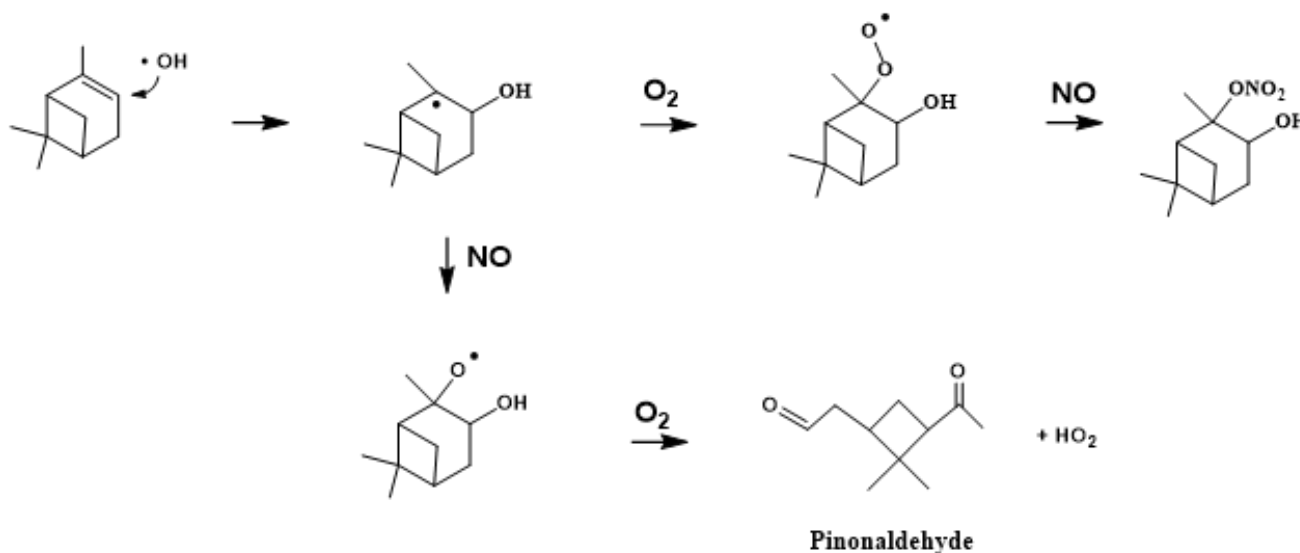
Figure 6: Example reaction pathways of the OH-initiated oxidation of α-pinene in the presence of NOₓ.
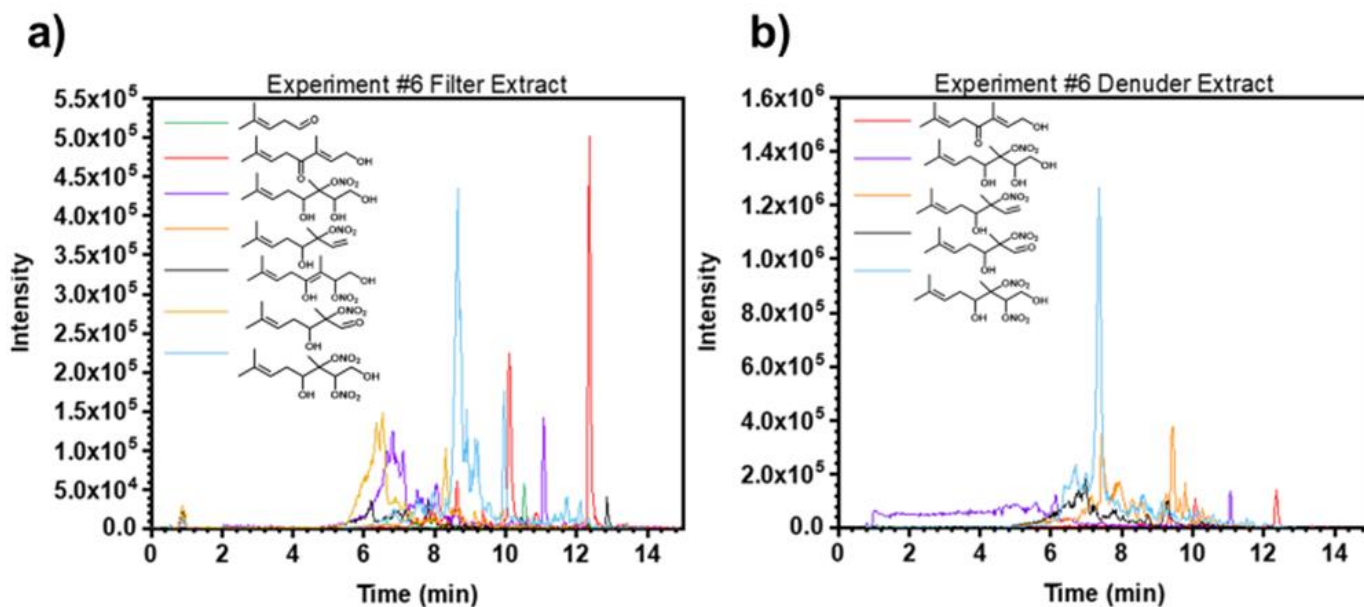
Figure 7: Selected ion chromatograms (SIC) of expected oxidation products in electrospray (ESI) negative mode for experiment #6 in the a) filter extract and b) denuder extract.
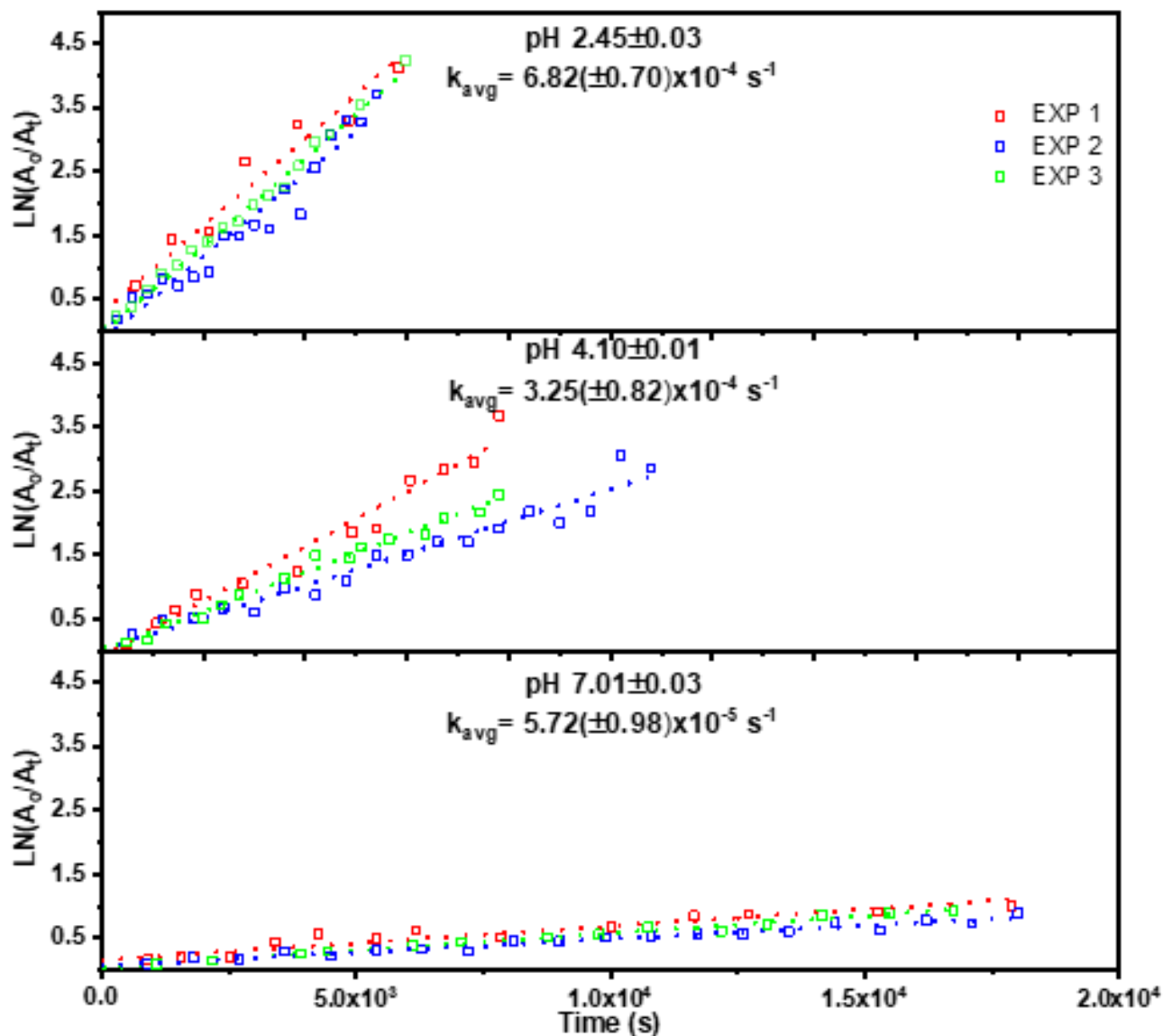
Figure 8: Hydrolysis rate constants for the bulk (gas- and particle-phase) organic nitrates at different pHs. Each pH was analyzed in triplicate and the k_{avg} is the average slope of each of the 3 trials.
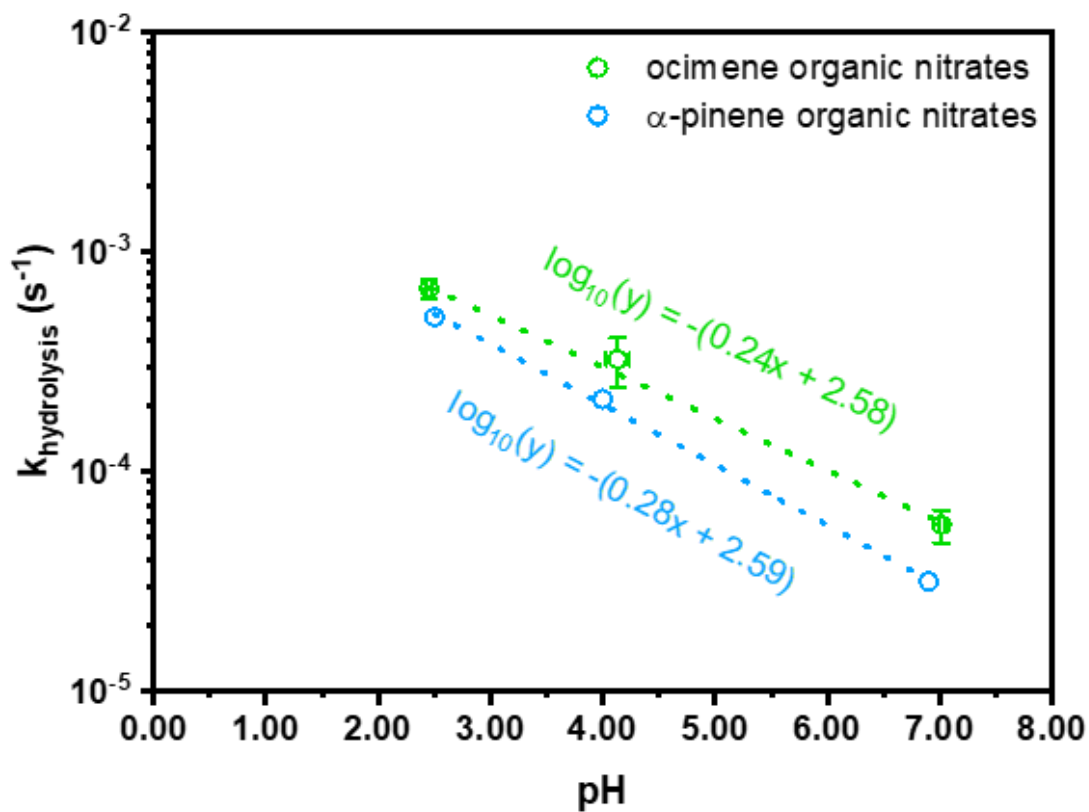
Figure 9: Hydrolysis rate constant for ocimene (this study, green) and alpha-pinene (Rindelaub et al., 2015, blue) as a function of pH.

Table 1: Experimental conditions and yield summary of individual experiments. Error represents the propagated analytical uncertainty.

Exp #	Seed	Irradiation time (min)	RH (%)	Δ [Ocimene] (ppb)	Δ [NO] (ppb)	Δ [NO$_2$] (ppb)	Δ [SOA mass] (μg m^{-3})	Gas phase - ONO$_2$ Yield (%)	Particle phase - ONO$_2$ Yield (%)	Hydroxynitrate Yield (%)
1	(NH$_4$)$_2$SO$_4$	19	<3%	266 ± 67	509 ± 57	475 ± 45	96 ± 10	nm	nm	nm
2	(NH$_4$)$_2$SO$_4$	54	<3%	223 ± 30	392 ± 29	284 ± 14	63 ± 5	nm	nm	nm
3[a]	(NH$_4$)$_2$SO$_4$	82	<3%	1357 ± 102	2604 ± 101	nm	933 ± 62	22% ± 5%	4.1% ± 1.1%	7(+2/-5)%
4	(NH$_4$)$_2$SO$_4$	73	<3%	425 ± 58	914 ± 13	587 ± 24	nm	27% ± 6%	1.5% ± 0.5%	6(+2/-4)%
5	(NH$_4$)$_2$SO$_4$	78	<3%	645 ± 49	1448 ± 11	817 ± 40	nm	35% ± 8%	1.6% ± 0.4%	nm
6	(NH$_4$)$_2$SO$_4$	82	<3%	516 ± 44	1540 ± 11	852 ± 33	143 ± 11	33% ± 8%	1.3% ± 0.3%	7(+2/-5)%
7	(NH$_4$)$_2$SO$_4$	102	<3%	524 ± 48	1091 ± 19	856 ± 33	189 ± 14	31% ± 7%	1.3% ± 0.3%	9(+2/-6)%
8	none	95	<3%	653 ± 45	1691 ± 11	1021 ± 38	101 ± 6	26% ± 6%	1.5% ± 0.4%	8(+2/-5)%
9	(NH$_4$)$_2$SO$_4$	92	46%	556 ± 44	1545 ± 52	1041 ± 38	238 ± 17	19% ± 4%	1.2% ± 0.3%	nm
10	(NH$_4$)$_2$SO$_4$	89	49%	692 ± 47	2019 ± 11	1185 ± 43	277 ± 24	18% ± 3%	0.9% ± 0.2%	7(+2/-5)%
11	none	19	<3 - 54%[b]	666 ± 38	nm	nm	BDL	13% ± 3%	BDL	6(+2/-4)%
12	(NH$_4$)$_2$SO$_4$	72	51%	798 ± 48	1913 ± 16	1034 ± 39	315 ± 23	18% ± 4%	1.0% ± 0.2%	3(+2/-2)%
13	(NH$_4$)$_2$SO$_4$	84	70%	641 ± 46	1628 ± 12	721 ± 41	269 ± 19	17% ± 3%	0.2% ± 0.2%	2(+1/-1.3)%
14	none	24	67%	407 ± 56	474 ± 11	90 ± 30	BDL	15% ± 3%	0.8% ± 0.2%	nm
15	(NH$_4$)$_2$SO$_4$	92	69%	783 ± 47	1643 ± 10	1209 ± 51	417 ± 26	13% ± 3%	0.8% ± 0.2%	nm
16	(NH$_4$)$_2$SO$_4$	86	13%	648 ± 49	nm	nm	238 ± 18	25% ± 6%	1.7% ± 0.5%	nm
17	(NH$_4$)$_2$SO$_4$	87	<3%	569 ± 41	1418 ± 20	878 ± 39	231 ± 18	32% ± 8%	1.8% ± 0.5%	nm
18	(NH$_4$)$_2$SO$_4$	88	<3%	560 ± 47	1256 ± 16	666 ± 27	156 ± 12	34% ± 8%	1.6% ± 0.4%	nm

a-high concentration experiment. Did not used for yield calculations; b-Irradiated under dry conditions, then increased RH in dark up to 54%

nm-not measured; BDL-below the detection limit